Nationaal Lucht- en Ruimtevaartlaboratorium
National Aerospace Laboratory NLR

Executive Summary

Extra-Large Eddy Simulations Using a High-Order Finite-Volume Scheme

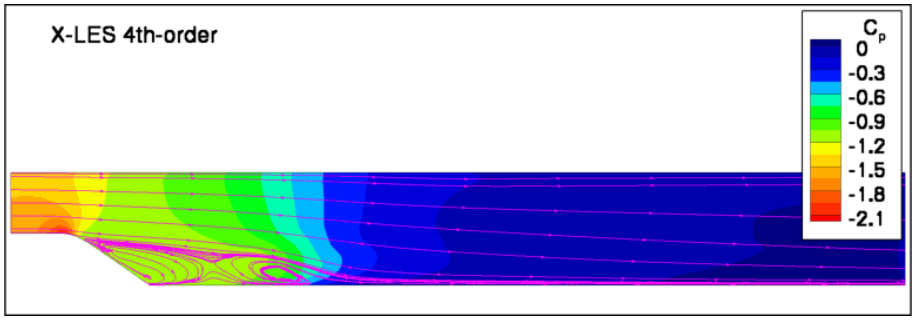

Problem area
Massively separated flows play an important role in topics such as the design of silent landing gear, the study of stability and control properties of fighter aircraft in relation to vortex breakdown, and the study of aerodynamic loads on structural aircraft components due to buffetting. These flows are strongly turbulent, involving a large range of spatial and temporal scales, which makes it difficult to model their dynamics with high physical accuracy and reliability. Flow computations based on the Reynold-averaged Navier–Stokes (RANS) equations are not able to capture the smaller turbulent scales. Large-eddy simulations (LES), on the other hand, do capture a signifcant range of scales, but are computationally too demanding for complex geometries. In recent years, therefore, research has focussed on hybrid RANS-LES methods, improving the physical accuracy compared to RANS, but without the cost of a full LES. In particular, NLR has developed the eXtra-Large Eddy Simulation (X-LES) method.

Description of work
The accuracy of a flow computation depends not only on the employed physical model, but also on the numerical method. In this paper, the impact on X-LES of a numerical method with fourth-order accuracy is considered. This high-order method prevents unphysical dissipation of the smaller turbulent structures inside the massively separated flows. Furthermore, the scheme preserves essential conservation and symmetry properties of the flow equations that are solved. A grid convergence study is performed for the separated flow over a rounded bump in a square duct, comparing the fourth-order method to a stan-

Report no.
NLR-TP-2007-800

Author(s)
J.C. Kok, B.I. Soemarwoto, and H. van der Ven

Classification report
Unclassified

Date
December 2007

Knowledge area(s)
Computational Physics & Theoretical Aerodynamics

Descriptor(s)
Hybrid RANS–LES
High-order finite-volume method
X-LES

This report is based on a presentation held at the Second Symposium on Hybrid RANS–LES Methods, Corfu, Greece, 17–18 June 2007 and that will be published in the Notes on Numerical Fluid Mechanics and Multidisciplinary Design, Vol. 97, Springer.

dard second-order method. Furthermore, the supersonic flow over a cavity is considered, which involves a shock wave. The fourth-order method is extended with a shock-capturing capability that maintains the high numerical accuracy in the separated flow regions.

Results and conclusions
The presented results show that the high-order method improves the numerical accuracy of the X-LES computations significantly. The fourth-order results are less sensitive to the grid resolution than the second-order results. The fourth-order method allows the mesh size to be at least twice as large as for the second-order method to obtain the same numerical accuracy. A standard method for computing shock waves is shown to be too dissipative in the separated flow regions. A modified approach, that can be combined with the high-order method, is shown to effectively resolve this problem.

Applicability
X-LES computations of massively separated flows will be performed with the high-order numerical method. This means that for the same computational cost, a numerically more reliable result can be obtained, compared to the second-order method.

Nationaal Lucht- en Ruimtevaartlaboratorium, National Aerospace Laboratory NLR

Anthony Fokkerweg 2, 1059 CM Amsterdam,
P.O. Box 90502, 1006 BM Amsterdam, The Netherlands
Telephone +31 20 511 31 13, Fax +31 20 511 32 10, Web site: www.nlr.nl

Nationaal Lucht- en Ruimtevaartlaboratorium
National Aerospace Laboratory NLR

NLR-TP-2007-800

Extra-Large Eddy Simulations Using a High-Order Finite-Volume Scheme

J.C. Kok, B.I. Soemarwoto and H. van der Ven

This report is based on a presentation held at the Second Symposium on Hybrid RANS-LES Methods, Corfu, Greece, 17-18 June 2007 and that will be published in the Notes on Numerical Fluid Mechanics and Multidisciplinary Design, Vol. 97, Springer.

This publication has been refereed by the Advisory Committee AEROSPACE VEHICLES.

Customer	NLR
Contract number	----
Owner	NLR
Division	Aerospace Vehicles
Distribution	Unlimited
Classification of title	Unclassified
	December 2007

Approved by:

Author	Reviewer	Managing department
30/1/2008	30/1/2008	30/1/2008

Summary

This paper focuses on numerical aspects for hybrid RANS–LES computations using the X-LES method. In particular, the impact of using a high-order finite-volume scheme is considered. The finite-volume scheme is fourth-order accurate on non-uniform, curvilinear grids, has low numerical dispersion and dissipation, and is based on the skew-symmetric form of the compressible convection operator, which ensures that kinetic energy is conserved by convection. A limited grid convergence study is performed for the flow over a rounded bump in a square duct. The fourth-order results are shown to depend only mildly on the grid resolution. In contrast, second-order results require at least half the mesh size to become comparable to the fourth-order results. Additionally, the high-order method is extended with a shock-capturing capability in such a way that interference with the subgrid-scale model is avoided. The suitability of this extension is demonstrated by means of a supersonic flow over a cavity.

Contents

1	Introduction	6
2	The X-LES method	7
3	High-order finite-volume method	7
4	Flow over a rounded bump in a square duct	8
5	Supersonic flow over a cavity	13
6	Conclusions	14
	Acknowledgments	16
	References	17

7 Figures

(17 pages in total)

1 Introduction

If a large-eddy simulation (LES) employs an explicit subgrid-scale (SGS) model, and one is interested in validating this model, then it is important to distinguish modelling errors from numerical errors. Typically, for a given numerical method, this is done by performing a grid convergence study. For LES, this requires that the SGS model is independent from the grid resolution, which can be obtained by fixing the filter width. In the context of hybrid RANS–LES computations, more often than not, second-order discretization methods are used. Performing a grid convergence study then easily leads to excessively fine grids, as second-order schemes typically require at least four grid cells per filter width (e.g., Vreman et al., 1997). Therefore, such grid convergence studies are seldom performed. Furthermore, in practice, often only one cell per filter width is used and it is likely that the results are strongly influenced by numerical errors from the second-order scheme.

To reduce the interference of numerical errors with the SGS model, the numerical accuracy of the scheme should be improved at wave lengths close to the filter width. These wave lengths are represented by only a few mesh widths and so the numerical accuracy is not determined by the order of the scheme, but rather by its dispersion and dissipation characteristics at large wave numbers. Numerical schemes optimized in that sense are, for example, the dispersion-relation preserving (DRP) scheme of Tam and Webb (1993) and the compact schemes of Lele (1992).

In this paper, a fourth-order finite-volume scheme with low numerical dispersion and dissipation is used for performing hybrid RANS–LES computations using the X-LES method (Kok et al., 2004). In particular, a high-order discretization of the convective operator is required, as shown, for example, by Kravchenko and Moin (1997). The finite-volume scheme is fourth-order accurate on non-uniform, curvilinear grids, has low numerical dispersion and dissipation, and is based on the skew-symmetric form of the compressible convection operator, which ensures that kinetic energy is conserved by convection (Kok, 2006). The accuracy of this finite-volume scheme has been assessed for a number of canonical test cases, including the convection of an isentropic vortex and the decay of isotropic, homogeneous turbulence. It was shown that the mesh size may be at least twice as large as for a second-order scheme to reach the same level of accuracy. It was also shown that, for the isentropic vortex, the skew-symmetric form reduces the numerical entropy errors by an order of magnitude. Thus, this scheme appears to be more amenable to performing grid convergence studies. A limited study is performed here for the flow over a rounded bump in a square duct, with the finest grid having two grid cells per filter width.

In more general cases, where a shock wave may be present in the flow, a particular numerical error that may easily dominate the SGS model is the numerical dissipation introduced by shock-capturing schemes. This issue is considered by means of the supersonic flow over a cavity.

2 The X-LES method

The X-LES formulation is a particular DES method (Spalart et al., 1997) that consists of a composition of a RANS k–ω turbulence model and a k-equation SGS model. Both models use the Boussinesq hypothesis to model the Reynolds or subgrid-scale stress tensor, which depends on the eddy-viscosity coefficient . Furthermore, both models are based on the equation for the modelled turbulent kinetic energy k, which depends on its dissipation rate ε. Both the eddy viscosity and the dissipation rate are modelled using the turbulent kinetic energy as velocity scale together with a length scale l_t,

$$\nu_t = l_t\sqrt{k} \qquad \text{and} \qquad \varepsilon = \beta_k \frac{k^{3/2}}{l_t} \tag{1}$$

where l_t is defined as a combination of the RANS length scale $l = \sqrt{k}/\omega$ and the SGS filter width Δ,

$$l_t = \min\{l, C_1\Delta\}, \tag{2}$$

with $C_1 = 0.05$. The RANS k–ω model is completed by an equation for the specific dissipation rate ω. The X-LES method will be in LES mode when the filter width (times C_1) is small compared to the RANS length scale. Note that in that case the SGS model is completely independent of ω.

3 High-order finite-volume method

In order to reduce the interference of numerical discretization errors with the subgrid-scale model, a high-order finite-volume scheme is employed. Details of this scheme are given by Kok (2006). In particular, the high-order scheme is used to discretize the inviscid terms of the flow equations. The diffusion terms (viscous terms and terms due to turbulence model) as well as the transport equations of the k–ω model are discretized with a standard second-order finite volume scheme. The high-order finite-volume scheme has the following key properties:

- It is formally fourth-order accurate. The order of accuracy is maintained on non-uniform curvilinear grids, provided they are sufficiently smooth. The finite-volume method has been made fourth-order accurate by extending the approach of Verstappen and Veldman (2003), which uses Richardson extrapolation, from Cartesian to curvilinear grids.

- The numerical dispersion of the scheme is minimized by extending the dispersion-relation preserving approach of Tam and Webb (1993) to finite-volume schemes.
- A central scheme is employed, containing no numerical dissipation. A small amount of sixth-order artificial diffusion is added explicitly to enhance stability. The artificial diffusion is scaled such that it introduces an error of only fifth order.
- The finite-volume approach leads to local conservation of mass, momentum, and energy.
- The discretization is based on the skew-symmetric form of the compressible convection operator in such a way that kinetic energy is exactly conserved by convection. For incompressible flow, this implies that the total kinetic energy cannot increase, ensuring numerical stability. For compressible flow, this is not the case (the total kinetic energy can increase due to work done by the pressure), but the advantage of the skew-symmetric form is that it does not lead to production or dissipation of kinetic energy interfering with the SGS model.

Although the high-order scheme is intended for the LES regions, it is applied throughout the complete flow domain. Thus, also the RANS region is solved with the fourth-order scheme. Others have proposed hybrid numerical schemes (Travin et al., 2002), in which a second-order upwind scheme is used in the RANS region. Although the fourth-order scheme is here used throughout, second-order accuracy is considered to be sufficient in the RANS region. Therefore, no effort has been made to develop a fourth-order accurate boundary condition at solid walls, and a second-order accurate boundary condition is used instead.

4 Flow over a rounded bump in a square duct

As first test case, the turbulent, separated flow over a rounded bump in a square duct (so-called ONERA bump) is considered. This is a standard DESider[1] test case for which experiments have been performed within the project by ONERA (Aupoix, 2007) in a hydraulic channel. The duct has a height of $0.3\,\mathrm{m}$, a width of $0.5\,\mathrm{m}$, and a length of $2.367\,\mathrm{m}$. The bump has a height of $0.138\,\mathrm{m}$, starts at the inflow plane at $x = -0.367\,\mathrm{m}$, and ends at $x = 0\,\mathrm{m}$. At the entrance, velocity profiles from the experiment are prescribed, which have a centre velocity of approximately $7\,{}^{\mathrm{m}}/_{\mathrm{s}}$. Furthermore, water with a density of $997\,{}^{\mathrm{kg}}/_{\mathrm{m}^3}$ and a dynamic viscosity of $0.89 \cdot 10^{-3}\,\mathrm{Pa} \cdot \mathrm{s}$ is considered. As a compressible flow solver is used for solving this incompressible flow, an inflow Mach number of $M = 0.1$ is chosen.

[1] DESider project (Detached Eddy Simulation for Industrial Aerodynamics) which is funded by the European Union

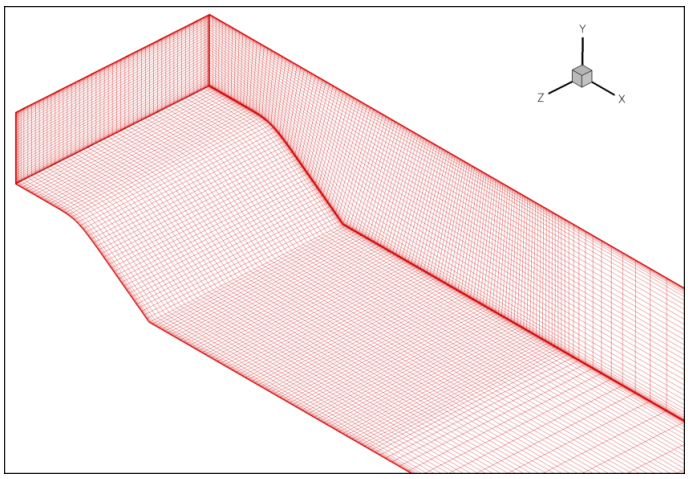

Fig. 1 ONERA bump: impression of geometry and grid (coarse level, i.e., showing every other grid point)

To study the grid dependence of the numerical schemes, a fixed filter width should be used, independent of the grid resolution. In this way, the SGS model is fixed and increasing the grid resolution will influence only the numerical errors and not the modelling errors. A coarse and a fine grid are considered, with the coarse mesh size equal to twice the fine mesh size. The filter width is defined as a factor times the maximum of the mesh size in the different computational directions, with the factor equal to one on the coarse grid and to two on the fine grid. In other words, per filter width, the coarse grid has one grid cell whereas the fine grid has two.

The fine grid has 284 cells in x-direction (streamwise), 120 cells in y-direction (height), and 152 cells in the z-direction (width), totalling $5\,180\,160$ cells (see Figure 1 for an impression). The grid outside the boundary layers is uniform from the inflow plane to $x = 0.6\,\mathrm{m}$. A time-step size is used of $\Delta t = 0.00189\,\mathrm{s}$, leading to a CFL number of approximately 2 in the uniform-grid region on the coarse grid. As the aim is here to look only at the effect of the spatial discretization on the results, the same time-step size is used for both grids. This means that the time-integration error is independent of the grid resolution, just like the SGS model. Therefore, although this error will influence the grid-converged solution, it will not affect the grid dependence of the solutions.

Computations are performed with both the second-order and the fourth-order schemes. Figure 2 shows the solution on the coarse grid in the centreplane $z = 0$, averaged over 2048 time steps ($3.87\,\mathrm{s}$). Clearly, the fourth-order result contains a larger separation region with the reattachment occurring further downstream and with a different streamline topology. This larger separation region is also present on the fine grid for both the second-order and fourth-order results

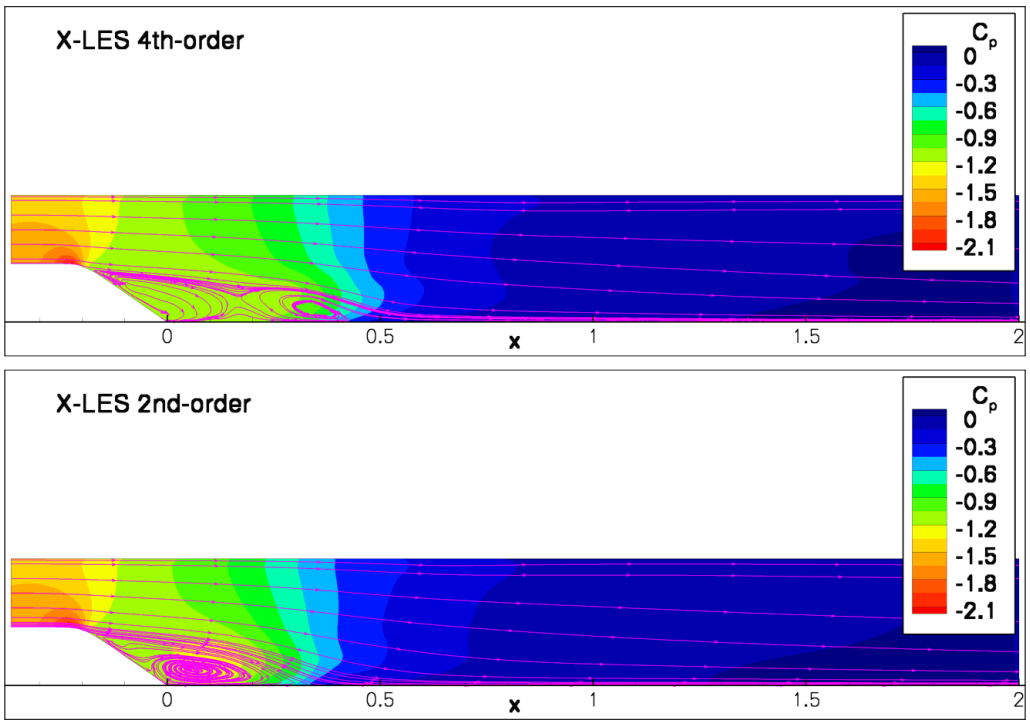

Fig. 2 ONERA bump: time-averaged pressure coefficient and streamlines on coarse grid in plane $z = 0$

(not shown), also averaged over 2048 time steps. This is also reflected in the pressure distribution along the bottom wall, given in Figure 3. The fourth-order result is closer to the experimental data, although a gap still remains. Moreover, for the fourth-order scheme, the coarse and fine-grid results are closer to each other than for the second-order scheme. In particular, in the smaller separation region, the second-order coarse-grid results show a low peak in the pressure coefficient (around $x = 0.1\,\mathrm{m}$) that is not present in the other results.

Profiles in the centreplane of the time-averaged velocity and of the resolved Reynolds stress are given in Figure 4 and Figure 5. The velocity profiles show that the second-order coarse-grid result reattaches around $x = 0.35\,\mathrm{m}$, the second-order fine-grid and fourth-order coarse-grid results around $x = 0.45\,\mathrm{m}$, the fourth-order fine-grid result just beyond that, and finally the experiment around $x = 0.625\,\mathrm{m}$. The fourth-order velocity profiles are closer to the experiment. In particular, before reattachment (of the X-LES results), the second-order results show fuller velocity profiles. Such profiles can be the effect of high levels of numerical dissipation in the second-order computations. For the profiles of resolved Reynolds stress, the second-order coarse-grid result deviates the most from the other results. In particular, the peak value is located at smaller values of y (closer to the wall), which is further away from the experiment. Surprisingly, at the

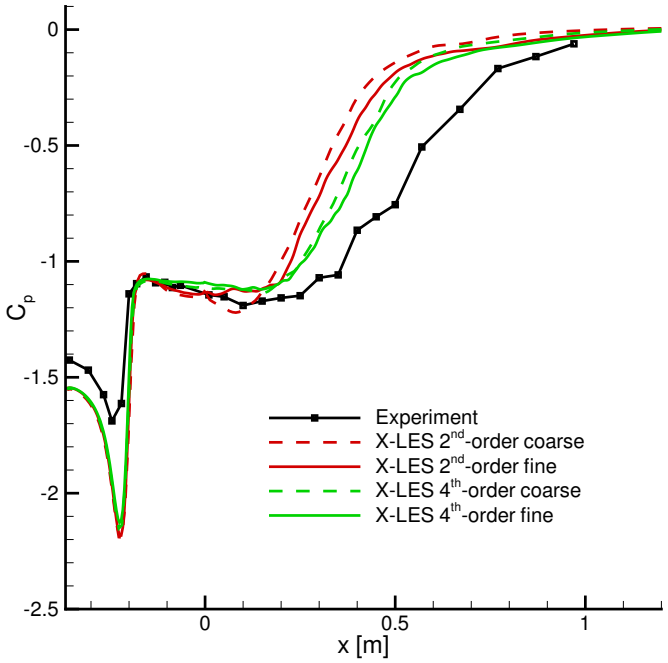

Fig. 3 ONERA bump: time-averaged pressure coefficient along centreline ($z = 0$) at bottom wall

first sections, the fourth-order fine-grid result shows the lowest level of resolved kinetic energy and the second-order coarse-grid result the highest. The level of resolved kinetic energy depends on the triggering of instabilities in the shear layer. Apparently, the result with the lowest numerical accuracy triggers the instabilities the first, possibly due to numerical disturbances.

Concerning the difference with the experimental results, similar differences were obtained by other partners in the DESider project, using a range of hybrid RANS–LES models. The difference in pressure level at inflow is caused by the difference in size and shape of the separation region, resulting in different losses in the tunnel and therefore in a different pressure jump between inflow and outflow. Critical for the size of the separation region is the rate at which the shear layer after the separation point becomes unstable. This rate appears to be lower in the computations than in the experiment. This is an aspect of hybrid RANS–LES models that needs further research. Another issue is the strength of the vortices along the side walls of the tunnels, which may be overpredicted in the computations.

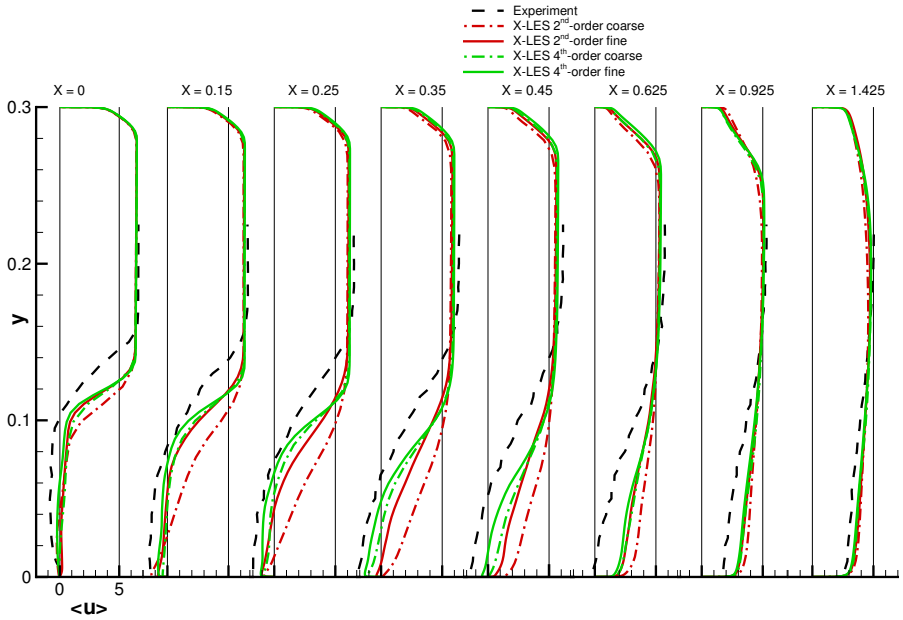

Fig. 4 ONERA bump: time-averaged velocity profiles (x-component) along cross sections in centreplane

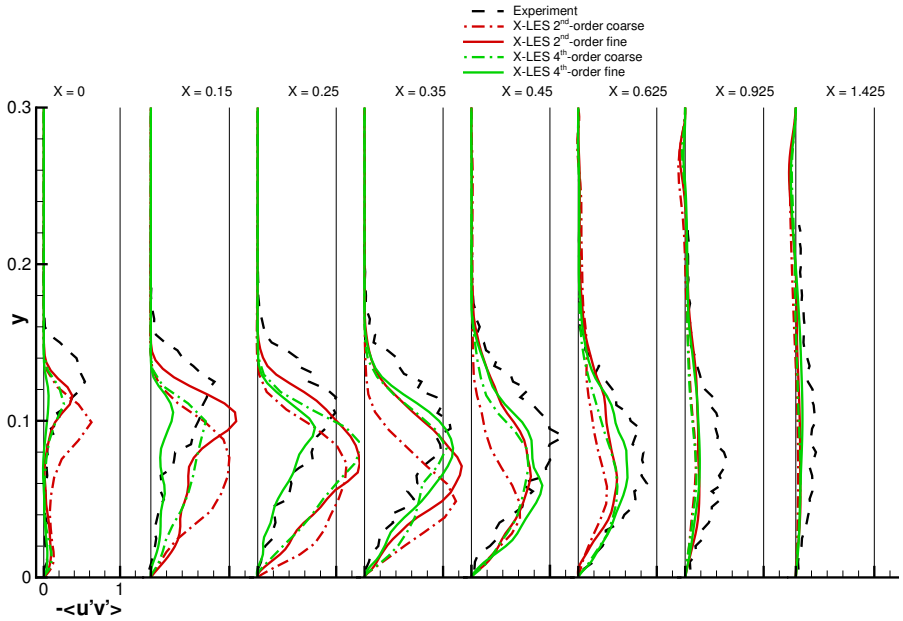

Fig. 5 ONERA bump: resolved Reynolds-stress profiles (xy-component) along cross sections in centreplane

5 Supersonic flow over a cavity

For transonic and supersonic flows including shock waves, the high-order scheme must be extended with a shock-capturing capability. Standard approaches, such as the Jameson scheme as well as upwind schemes, will give rise to high levels of numerical dissipation away from shocks that may completely swamp the subgrid-scale model. Here, the standard Jameson scheme is considered. A blending of second-order and sixth-order artificial diffusion is added to the scheme, where the second-order diffusion is switched on near shocks using a pressure-based shock sensor. For the momentum equation, the second-order artificial diffusion in the x-direction can be written as

$$\frac{\partial}{\partial x}\left(\nu_a \frac{\partial(\rho \boldsymbol{u})}{\partial x}\right), \tag{3}$$

in which ν_a is an artificial viscosity coefficient given by

$$\nu_a = s(|u| + c)\Delta x, \tag{4}$$

with s the shock sensor, u the x-component of velocity, c the speed of sound, and Δx the mesh size. This artificial viscosity should be small compared to the eddy viscosity. For the standard Jameson sensor,

$$s_J = \frac{|p_{i+1} - 2p_i + p_{i-1}|}{p_{i+1} + 2p_i + p_{i-1}} \tag{5}$$

(with i the grid index), the artificial viscosity is $O((\Delta x)^3)$ in smooth flow regions. Thus, the numerical scheme will only be third-order accurate. Therefore, the following modification is considered,

$$s = \min\{20 s_J^2, s_J\}, \tag{6}$$

for which the artificial viscosity is $O((\Delta x)^5)$ and which restores the fourth-order accuracy of the scheme in smooth flow regions. Furthermore, the value of the sensor in the shock ($s_J \geq 0.05$) is maintained.

To assess the high-order scheme including the shock-capturing capability, the supersonic flow over a cavity is considered. The cavity has length-to-depth and length-to-width ratios $L/D = L/W = 4.5$ (open cavity), a free-stream Mach number $M = 1.5$, and a Reynolds number $Re_L = 4.5 \cdot 10^6$. The domain inside the cavity is represented by $524\,288$ grid cells, consisting of a single block with a near-uniform grid of $192 \times 32 \times 32$ cells, surrounded by blocks with stretched grids to capture the near-wall layers.

X-LES computations are performed with the filter width defined as the maximum of the mesh size in the different computational directions. An (unconverged) steady computation is used as the initial solution. Both the second-order and the fourth-order scheme are blended with the Jameson shock-capturing scheme as explained above. The main question is to what extent the second-order artificial diffusion interferes with the subgrid-scale model.

In Figure 6 and Figure 7, the solutions are compared after 64 time steps of size $\Delta t = 0.0812 L/u_\infty$. The pressure contours in subfigures (a) clearly show an oblique shock wave structure. Subfigures (b) show the ratio of the artificial viscosity ν_a and the eddy viscosity ν_t in the region where the flow can be considered turbulent ($\nu_t > \nu_\infty$). For the second-order scheme, the standard Jameson shock sensor is used. There is clearly a strong interference of the artificial diffusion with the subgrid-scale model. In a large part of the cavity, the artificial viscosity is of the same order or even larger than the eddy viscosity. For the fourth-order scheme, using the modified 'fourth-order' shock sensor, the situation improves strongly. In most part of the cavity the artificial viscosity is negligible compared to the eddy viscosity. If two cells are used per filter width, then the ratio of artificial and eddy viscosity is reduced further by a factor $2^5 = 32$ (as it scales with $(\Delta x)^5$ in smooth flow regions).

Thus, it appears to be feasible to blend the high-order scheme with a shock-capturing scheme, without numerical dissipation interfering with the subgrid-scale model.

6 Conclusions

X-LES computations using fourth-order and second-order finite-volume schemes have been presented. For the flow over a rounded bump in a square duct, the fourth-order results are clearly superior to second-order results, showing weaker grid dependence. Consistent with previous results for canonical test cases, it appears that for the fourth-order scheme the mesh sizes may be twice as large as for the second-order scheme to reach the same level of numerical accuracy. It is likely that computations with a second-order scheme and with one grid cell per filter width, as is commonly the case for hybrid RANS–LES computations, suffer from numerical errors interfering with the subgrid-scale model. This is more so if a standard shock-capturing scheme is used, including some form of second-order numerical dissipation, as has been shown for the supersonic flow over a cavity. For the Jameson scheme, a simple modification has been proposed so that the scheme can be used in combination with the fourth-order finite-volume scheme, while leaving the order of accuracy away from shocks intact.

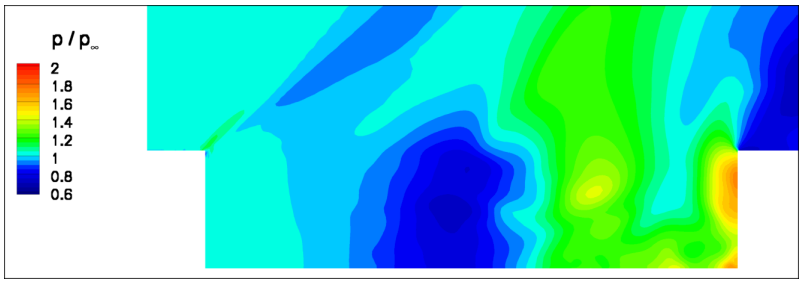

(a) Pressure

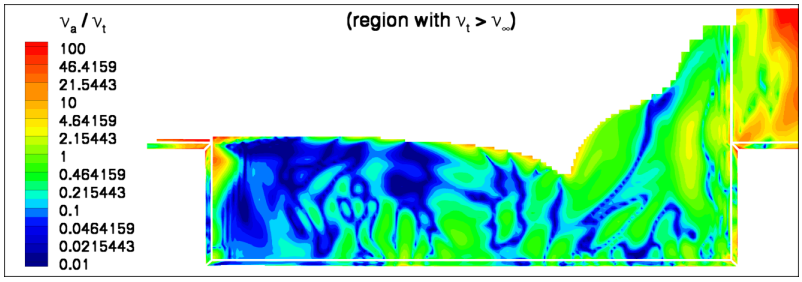

(b) Ratio of artificial and eddy viscosity coefficients for the artificial diffusion in the first computational direction (approximately x direction)

Fig. 6 Flow over cavity: Second-order scheme's solution in the centre plane after 64 time steps ($Re_L = 4.5 \cdot 10^6$, $M = 1.5$)

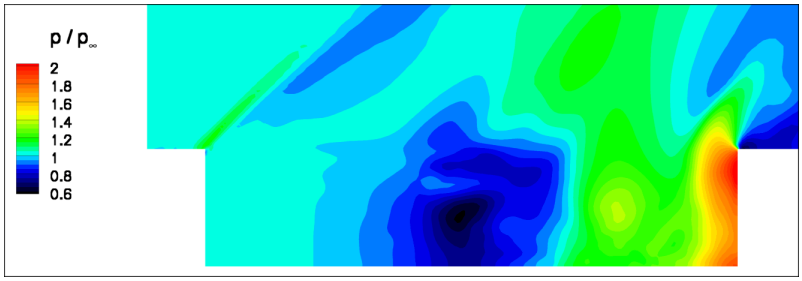

(a) Pressure

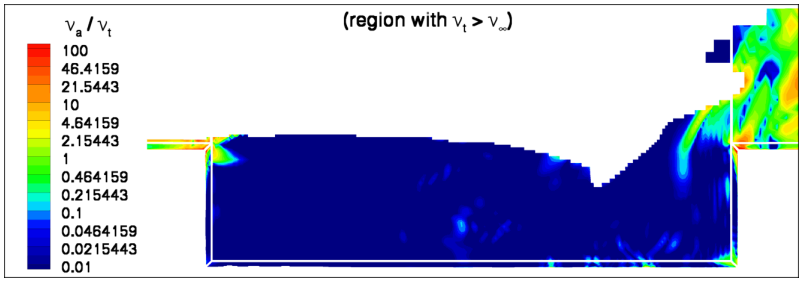

(b) Ratio of artificial and eddy viscosity coefficients for the artificial diffusion in the first computational direction (approximately x direction)

Fig. 7 Flow over cavity: Fourth-order scheme's solution in the centre plane after 64 time steps ($Re_L = 4.5 \cdot 10^6$, $M = 1.5$)

Acknowledgments

This work was partially performed within the EU project DESider (Detached Eddy Simulation for Industrial Aerodynamics), which is funded by the European Union under Contract No. AST3-CT-2003-502842 of the European Commission, and partially within NLR's Programmatic Research Programme.

References

B. Aupoix. The DESider bump experiment for hybrid modelling validation. In *EWA workshop*, Prague, 5–6 June 2007.

J. C. Kok. A symmetry and dispersion-relation preserving high-order scheme for aeroacoustics and aerodynamics. In P. Wesseling, E. Oñate, and J. Périaux, editors, *ECCOMAS CFD 2006*, Egmond aan Zee, The Netherlands, 5–8 September 2006. NLR-TP-2006-525.

J. C. Kok, H. S. Dol, B. Oskam, and H. van der Ven. Extra-large eddy simulation of massively separated flows. In *42nd AIAA Aerospace Sciences Meeting*, Reno, NV, 5–8 January 2004. AIAA paper 2004-264.

A. G. Kravchenko and P. Moin. On the effect of numerical errors in large eddy simulations of turbulent flows. *Journal of Computational Physics*, 131:310–322, 1997.

S. K. Lele. Compact finite difference schemes with spectral-like resolution. *Journal of Computational Physics*, 103(1):16–42, 1992.

P. R. Spalart, W.-H. Jou, M. Strelets, and S. R. Allmaras. Comments on the feasibility of LES for wings, and on a hybrid RANS/LES approach. In C. Liu and Z. Liu, editors, *Advances in DNS/LES*. Greyden Press, 1997. Proc. 1st AFOSR Int. Conf. on DNS/LES, 1997, Ruston (LA), USA.

C. K. W. Tam and J. C. Webb. Dispersion-relation-preserving finite difference schemes for computational acoustics. *Journal of Computational Physics*, 107:262–281, 1993.

A. Travin, M. Shur, M. Strelets, and P. R. Spalart. Physical and numerical upgrades in the detached-eddy simulation of complex turbulent flows. In R. Friedrich and W. Rodi, editors, *Advances in LES of Complex Flows*, pages 239–354. Kluwer Academic Publishers, 2002. Proc. of the Euromech Colloquium 412, 2000, Munich, Germany.

R. W. C. P. Verstappen and A. E. P. Veldman. Symmetry-preserving discretization of turbulent flow. *Journal of Computational Physics*, 187(1):343–368, 2003.

B. Vreman, B. Geurts, and H. Kuerten. Large-eddy simulation of the turbulent mixing layer. *Journal of Fluid Mechanics*, 339:357–390, 1997.